

Article

TP-CSO: A Triptolide Prodrug for Pancreatic Cancer Treatment

Xinlong Wang^{1,2}, Huahui Zeng¹, Xin Zhu², Duanjie Xu², Qikang Tian², Can Wang², Lingzhou Zhao³, Junwei Zhao⁴, Mingsan Miao^{1,2,*} and Xiangxiang Wu^{1,2,*} 

- ¹ Academy of Chinese Medicine Sciences, Henan University of Chinese Medicine, Zhengzhou 450046, China; wangxl_115@126.com (X.W.); hhzeng@hactcm.edu.cn (H.Z.)
- ² Pharmacy College, Henan University of Chinese Medicine, Zhengzhou 450046, China; xerz2@126.com (X.Z.); xudianjie123@163.com (D.X.); hucmkang@163.com (Q.T.); wangjiucan@163.com (C.W.)
- ³ Department of Nuclear Medicine, Shanghai General Hospital, Shanghai Jiao Tong University School of Medicine, Shanghai 200080, China; zlz-330@163.com
- ⁴ Department of Clinical Laboratory, The First Affiliated Hospital of Zhengzhou University, Zhengzhou 450052, China; junweizhao@alumni.sjtu.edu.cn
- * Correspondence: miaomingsan@163.com (M.M.); wuxx-415@hactcm.edu.cn (X.W.); Tel.: +86-0371-6568-0206 (X.W.)

Abstract: Triptolide (TP) is a potential drug candidate for the treatment of cancer, but its use was hampered by its systemic toxicity and poor water solubility. Hence, a TP-CSO prodrug was synthesized by conjugating TP to chitosan oligosaccharide (CSO), and characterized by ¹H NMR, FTIR, DSC and XRD analyses. The TP-CSO containing about 4 wt% of TP exhibited excellent water solubility (15 mg/mL) compared to TP (0.017 mg/mL). Compared with TP, the pharmacokinetics of the conjugate after oral administration showed a three-fold increase in the half-life in the blood circulation and a 3.2-fold increase in AUC_(0-∞). The orally administered TP-CSO could more effectively inhibit tumor progression but with much lower systemic toxicity compared with TP, indicating significant potential for further clinical trials. In conclusion, CSO-based conjugate systems may be useful as a platform for the oral delivery of other sparingly soluble drugs.



Citation: Wang, X.; Zeng, H.; Zhu, X.; Xu, D.; Tian, Q.; Wang, C.; Zhao, L.; Zhao, J.; Miao, M.; Wu, X. TP-CSO: A Triptolide Prodrug for Pancreatic Cancer Treatment. *Molecules* **2022**, *27*, 3686. <https://doi.org/10.3390/molecules27123686>

Academic Editor: Silvia Arpicco

Received: 18 May 2022

Accepted: 6 June 2022

Published: 8 June 2022

Publisher's Note: MDPI stays neutral with regard to jurisdictional claims in published maps and institutional affiliations.



Copyright: © 2022 by the authors. Licensee MDPI, Basel, Switzerland. This article is an open access article distributed under the terms and conditions of the Creative Commons Attribution (CC BY) license (<https://creativecommons.org/licenses/by/4.0/>).

Keywords: triptolide; toxicity; water solubility; pharmacokinetics; pancreatic cancer

1. Introduction

Pancreatic cancer (PC) is a malignant tumor of the digestive tract. The morbidity and mortality of PC rank among the top of malignant tumors [1–3]. Currently, GNP (gemcitabine with albumin-bound paclitaxel) and FOLFIRINOX (5-fluorouracil, leucovorin, irinotecan, and oxaliplatin) has been widely used as first-line chemotherapy regimens for the treatment of advanced pancreatic cancer [4,5]. However, pancreatic cancer can evade cell death due to its potential drug resistance, so the clinical effectiveness of this treatment isn't satisfactory [6,7]. Therefore, it is of great significance to develop a drug that can reduce drug resistance to pancreatic cancer and improve its tumor suppressive effect.

Triptolide (TP) is one of the main bioactive ingredients of *Tripterygium wilfordii* Hook F (TWHF) in the Euonymus family. Recently, TP has attracted immense attention to its anticancer activity with multiple mechanisms, which can reduce drug resistance for cancers [8–11]. Several studies have shown that TP is more effective against pancreatic cancer compared with gemcitabine, paclitaxel, cisplatin and doxorubicin [12–14]. However, its clinical development has been greatly hampered by its poor water solubility (0.017 mg/mL) [15], multi-organ toxicity [16–18] and low bioavailability.

Recently, a polysaccharide has been developed adequately as a carrier for the clinical application of hydrophobic drugs. The chemotherapy drug-conjugated chitosan, such as LMWC-DTX, LMWC-PTX, exhibited superior antitumor efficacy and less toxicity compared with the parent paclitaxel (docetaxel) [19,20]. Chitosan is a biocompatible, biodegradable, and low-toxic natural polysaccharide. Drug delivery vehicles based on various derivatives

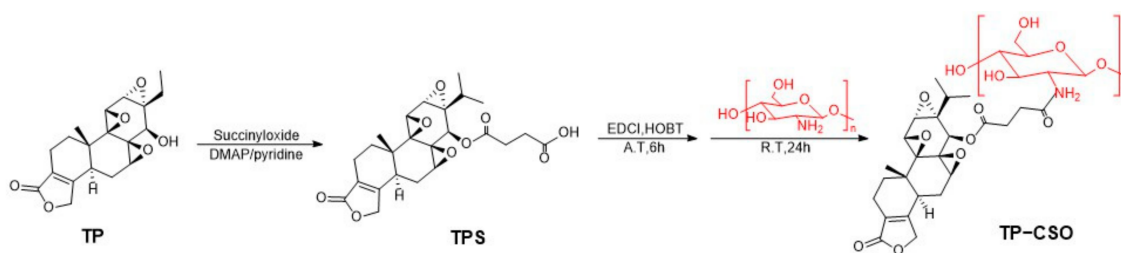
of chitosan are currently being explored. Recently, we reported on an oral triptolide-conjugated carboxymethyl chitosan prodrug (CCTP), in which CC acted as a carrier [21]. The CCTP conjugate showed better water solubility (5 mg/mL), lower toxicity, but slightly weaker anticancer effect than the free TP. Chitosan oligosaccharide (CSO, MW: about 3000 Da), low molecular weight chitosan, exhibits nontoxicity, better water-solubility, and a high rate of assimilation in the human gastrointestinal tract [22]. Thus, chitosan oligosaccharide was used as a drug carrier to develop a triptolide-conjugated CSO prodrug (TP-CSO). In our work, we hypothesized that TP-CSO might display several advantages for oral administration, including by dramatically enhancing the water solubility of TP, the significantly reduced toxicity of TP, the prolonged retention of the drug in the blood, and the improved bioavailability and antitumor efficacy *in vivo*.

Usually, the TP-CSO conjugate may differ from its parent TP in terms of its pharmaceutical efficacy and physicochemical properties. Here we describe the synthesis, characterization, and *in vitro* drug release profiles of TP-CSO conjugates with preliminary evaluation in mice, aiming to develop a technological platform for the oral delivery of TP.

2. Results and Discussion

2.1. Preparation and Characterization of TP-CSO

As shown in Scheme 1, TP-CSO was prepared by a coupling reaction between TPS and CSO, and TP could be released via hydrolysis. The structure information of TP, CSO, TP+CSO (physical mixture) and TP-CSO was shown in Figure 1 (^1H NMR see Supplementary Materials, Figure S1). TP shows a strong absorption band at 1748.56 cm^{-1} that was associated with the C=O stretching of cyclic ester groups. The characteristic peaks of the CSO at 3399.62 cm^{-1} was due to the stretching vibration of NH_2 and OH groups. Moreover, the 1617.48 cm^{-1} absorption band was corresponded to the N-H deformation of amino groups. The FTIR spectra of TP-CSO showed a new absorption peak at the wavenumbers of 1643.05 cm^{-1} , which is attributed to the C=O stretching vibration of the amide group, while the absorption band at the wavenumber of 1617.48 cm^{-1} (corresponding to the NH_2 group of CSO) mostly disappeared in the FTIR spectrum of TP-CSO, which indicated that the amide group was successfully introduced (Figure 1A).



Scheme 1. Schematic illustration of the synthetic pathway of TPS and TP-CSO conjugate.

The thermal behaviors of TP, CSO, TP-CSO and physical mixture (TP+CSO) were investigated using DSC under a nitrogen atmosphere (Figure 1B). The exothermic peaks of the CSO and physical mixture (containing 4 wt% of TP and 96 wt% of CSO) were in the range of $67\text{--}71\text{ }^\circ\text{C}$. However, the free TP showed a sharp exothermic peak at $213.1\text{ }^\circ\text{C}$ and a broad endothermic peak at $239.6\text{ }^\circ\text{C}$, respectively. The TP-CSO conjugate displayed a broad endothermic peak at $227.04\text{ }^\circ\text{C}$ with an onset at $209.03\text{ }^\circ\text{C}$ (Figure 1C). Thus, the endotherm of TP-CSO reflected the physical and chemical structure changes during the introduction of the TP moiety into the CSO backbone. In addition, the physical mixture and CSO had the enthalpy (ΔH) of -188.41 J/g , whereas TP-CSO had ΔH of 73.56 J/g (Figure 1C). This result could be explained by the fact that increasing acylation caused an increase in enthalpy, which was consistent with the previous report [23]. The XRD patterns of TP, CSO, TP-CSO and the physical mixture (TP+CSO) were depicted in Figure 1D. TP showed many small XRD peaks between the 2θ range of $9.54\text{--}28.69^\circ$, whereas CSO exhibited two continuous peaks at 21.47° and 24.56° . Compared with TP and CSO, the

physical mixture (containing 4 wt% of TP and 96 wt% of CSO) displayed the multiple XRD peaks from the overlap between TP and CSO. Therefore, the broad single XRD patterns of the TP-CSO reflected the decrease in crystallinity of the TP-CSO backbone, which could be attributed to the presence of TP moiety. The XRD patterns revealed that TP-CSO were amorphous compared to TP and CSO. Furthermore, the result indicated that the TP moiety was successfully introduced into the CSO backbone.

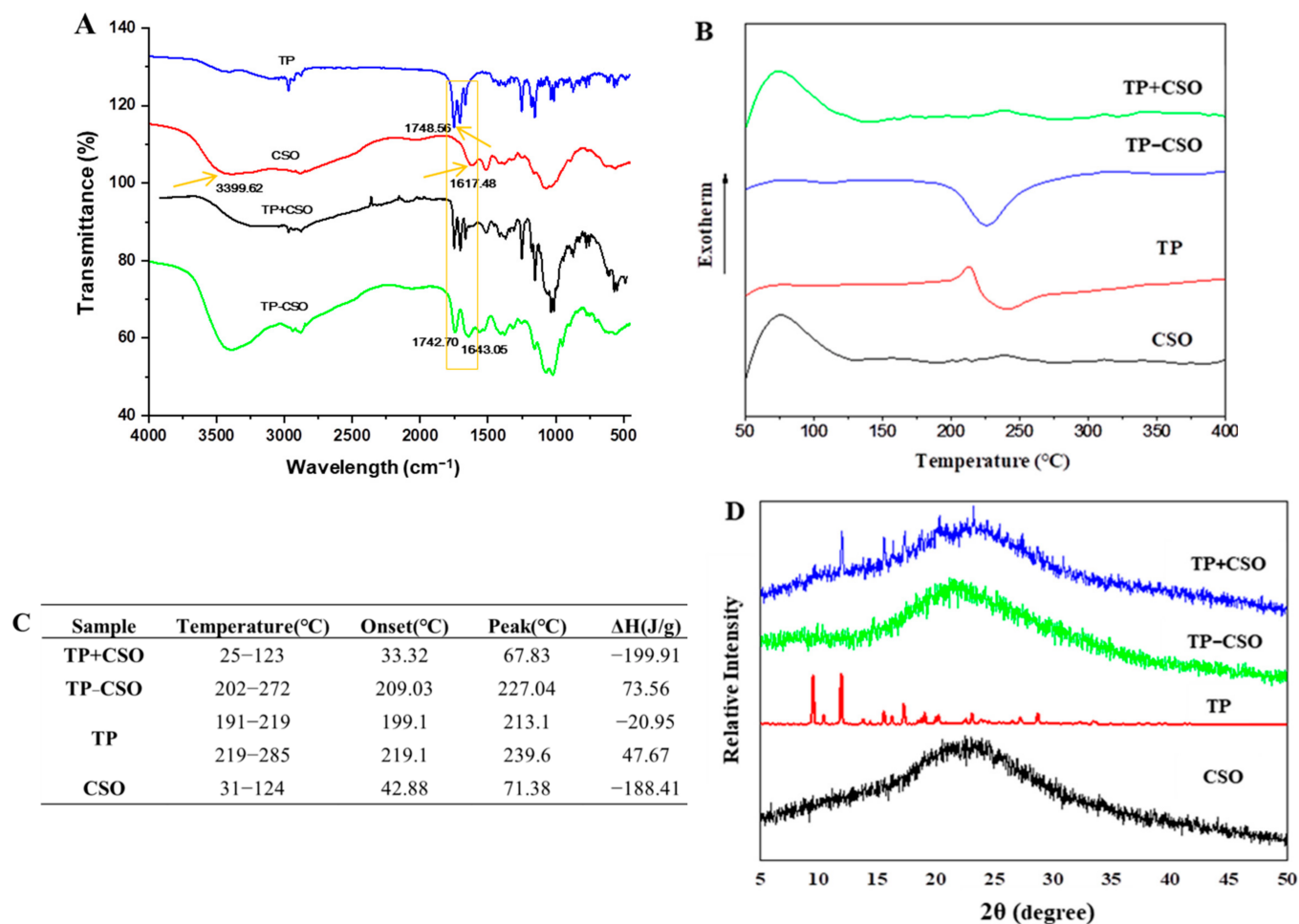


Figure 1. FTIR spectra of TP, CSO, TP+CSO, TP-CSO (A); DSC thermogram patterns of TP, CSO, TP+CSO, TP-CSO (B); DSC data of TP, CSO, TP+CSO, and TP-CSO (C); XRD diffraction patterns of TP, CSO, TP+CSO, and TP-CSO (D).

The weight percentage of TP in TP-CSO was measured at approximately 4 wt% by using the HPLC method (for HPLC spectra see Supplementary Materials, Figures S2 and S3). The TP-CSO conjugate, a yellowish solid, has over a 35-fold greater water solubility (15 mg TP-CSO/mL) than TP (0.017 mg/mL). The above results showed that the TP-CSO conjugate had been successfully synthesized through the coupling of TP and CSO, which significantly improved the water solubility of TP.

In order to investigate the *in vitro* release behavior of TP-CSO, we measured the drug release of TP-CSO in mouse plasma, cell culture medium, SGF, and SIF at 37 °C (Figure 2). The TP released from TP-CSO was detected by the HPLC in different solutions, which had the same retention time as the native TP, showing that the ester bonds between TP and CSO were cleaved by enzymatic attack. A small amount of TP released from the TP-CSO conjugate was observed after 24 h post incubation in cell culture medium (12.45%), SGF (8.81%) and SIF (6.41%), while 87.58% of TP was observed after 24 h incubation in mouse plasma. The results showed that TP-CSO was quite stable in the cell culture media SGF and SIF, but was easily hydrolyzed in mouse plasma. Owing to the low drug release in

SGF and SIF, TP release in SGF and SIF would seem insubstantial, indicating that most of the TP release did not take place in the gastric or intestinal environment, but might mainly transport to the blood capillary.

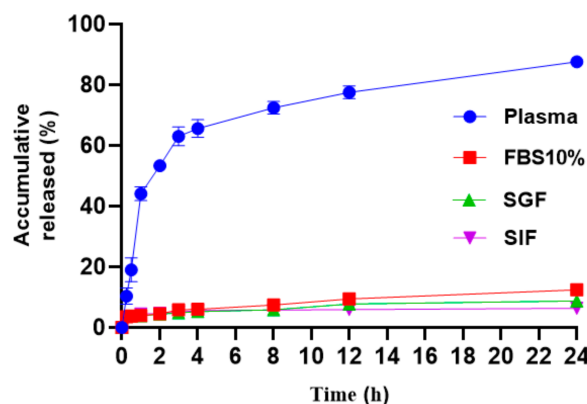


Figure 2. TP-CSO release profiles in mouse plasma, 10% FBS of cell culture medium, SGF (simulated gastric fluid, pH 1.2), and SIF (simulated intestinal fluid, pH 7.5) ($n = 3$).

2.2. Pharmacokinetics after Gavage Administration of TP-CSO to Rats

The pharmacokinetic parameters after gavage administration of TP and TP-CSO in rats were investigated by the LC-MS method to quantify the plasma level of the free TP. As shown in Figure 3A, two concentration curves of TP exhibited a rapid increase, followed by a slow decrease. Meanwhile, the TP-CSO group showed higher detectable concentrations compared with the TP group over a long period of time, suggesting that TP-CSO has higher gastrointestinal absorption and sustained TP release. The relevant pharmacokinetic parameters (e.g., T_{max} , C_{max} , $t_{1/2}$ and $AUC_{0-\infty}$) are shown in Figure 3B. The peak time (T_{max}) of TP was half shorter than that of TP-CSO, whereas the peak concentration (C_{max}) of the conjugate was five-fold higher than that of TP. In addition, the apparent half-life of TP-CSO ($t_{1/2} = 127.62$ min) was three times longer in the plasma than that of TP ($t_{1/2} = 42.62$ min), indicating TP-CSO showed a slow clearance of TP from the blood. The $AUC_{0-\infty}$ of TP-CSO (0.196 ng·h/mL) was over three times higher than that of TP (0.061 ng·h/mL), suggesting a high absorption of TP-CSO, which may be attributed to the increase of its water solubility and the high absorption rate of CSO in the gastrointestinal tract.

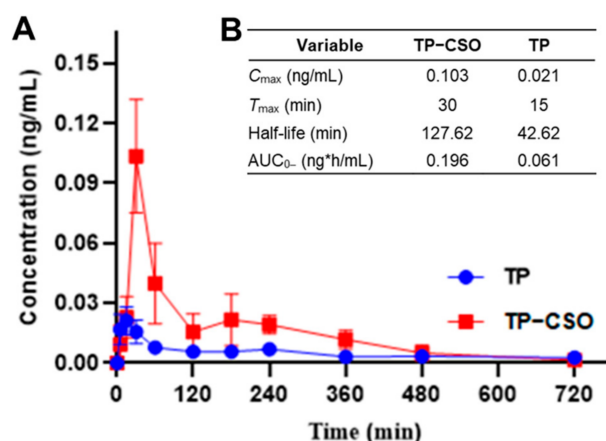


Figure 3. Plasma concentration of TP (A), pharmacokinetic parameters (B) after administration of TP and TP-CSO, respectively ($n = 5$).

2.3. In Vivo Toxicity of TP-CSO

The in vivo toxicity of TP and TP-CSO was evaluated in healthy C57 mice (Figure 4A). According to our preliminary experiments, the minimum dose of TP causing the death of mice was about 0.6 mg/kg. There was no significant difference in body weight between

the low- and medium-dose TP-CSO groups and the control group ($p < 0.05$), while the TP group and the high-dose TP-CSO group showed obvious body weight loss but without lethality at the end of the experiment, indicating that TP-CSO protected mice from weight loss or death caused by TP-induced toxicity.

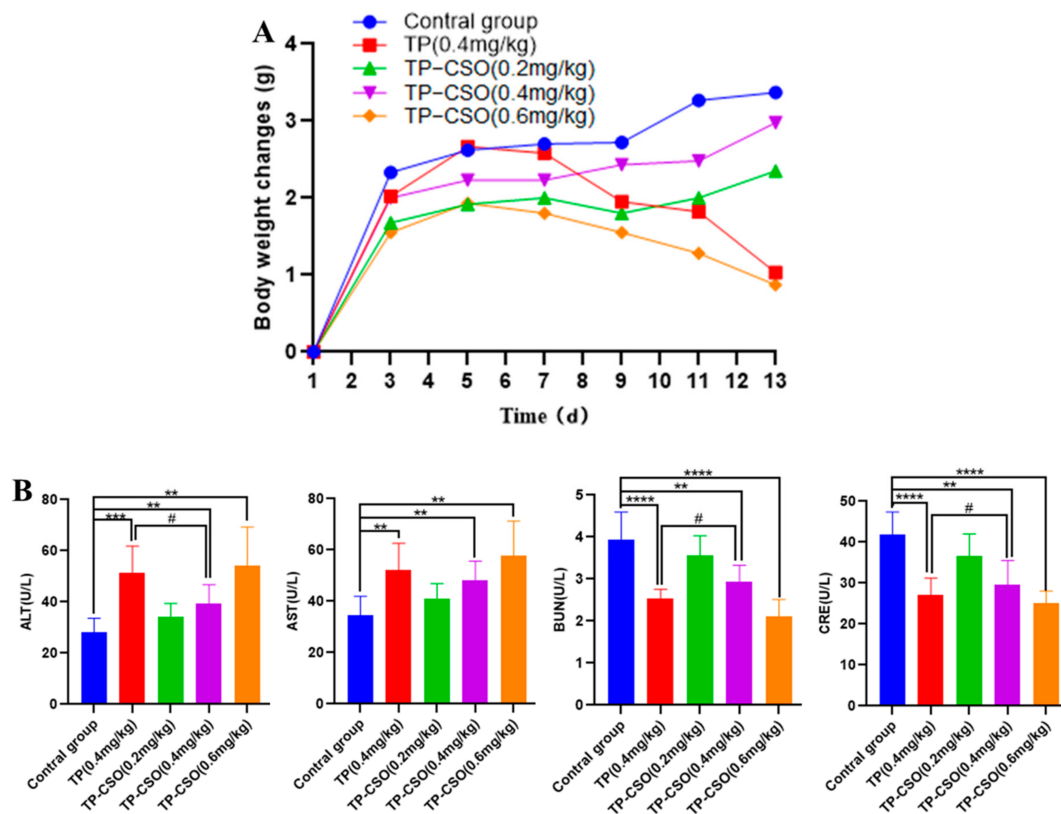


Figure 4. In vivo toxicity of TP and TP-CSO: body weight changes (A); biochemical parameters (B). ** Represents $p < 0.01$, *** represents $p < 0.001$, **** represents $p < 0.0001$, vs. control group; # represents $p < 0.0001$, TP-CSO (0.4 mg/kg) vs. TP group (0.4 mg/kg) ($n = 6$).

Different degrees of liver and kidney injury are indicated by the changes in serum ALT, AST, BUN and CRE levels [24]. The ALT and AST levels in the TP group and the high-dose TP-CSO group were obviously higher than those in other groups, which indicated the two groups occurred liver injury ($p < 0.05$, Figure 4B). However, the low- and medium-dose of TP-CSO groups showed moderate effects on ALT and AST in comparison to the control group ($p < 0.05$), which were still safe for the liver. In the TP group and high-dose TP-CSO group, BUN and CRE levels were significantly lower than in the control group (Figure 4B). The low-dose TP-CSO group had a slight effect on BUN and CRE, whereas the medium-dose TP-CSO group showed higher BUN and CRE levels in comparison to the TP group. The study results showed that in vivo toxicity of TP is related to hepatic and renal injury in a dose-dependent manner. As compared with the TP group, the medium-dose TP-CSO group underwent mild changes in AST, ALT, BUN and CRE levels, indicating that TP-CSO may relieve the TP-induced toxicity in liver and kidney.

2.4. Antitumor Activity of TP-CSO

The in vivo antitumor efficacy of TP-CSO was assessed by monitoring changes of tumor volume in the Panco2-bearing mice (Figure 5). The tumor volume gradually increased in all treatment groups for the first seven to nine days, followed by a decrease in tumor volume (Figure 5A). Compared to the control group, the tumor in all treated groups was significantly diminished in the dose-dependent manner ($p < 0.05$), especially in the high-dose TP-CSO group (Figure 5B). By the end of the study, the tumor-inhibition rate

(TIR) was 43.39% in the TP group, 42.18%, 59.23%, and 90.29% in the low-, medium-, and high-dose TP-CSO groups, respectively. At the same dose of TP, TP-CSO had a stronger tumor inhibition effect than the free TP, indicating that much more TP-CSO conjugate were actively or passively accumulated in the tumor cells, followed by TP release from the conjugate via cleavage of the succinate linker between TP and CSO.

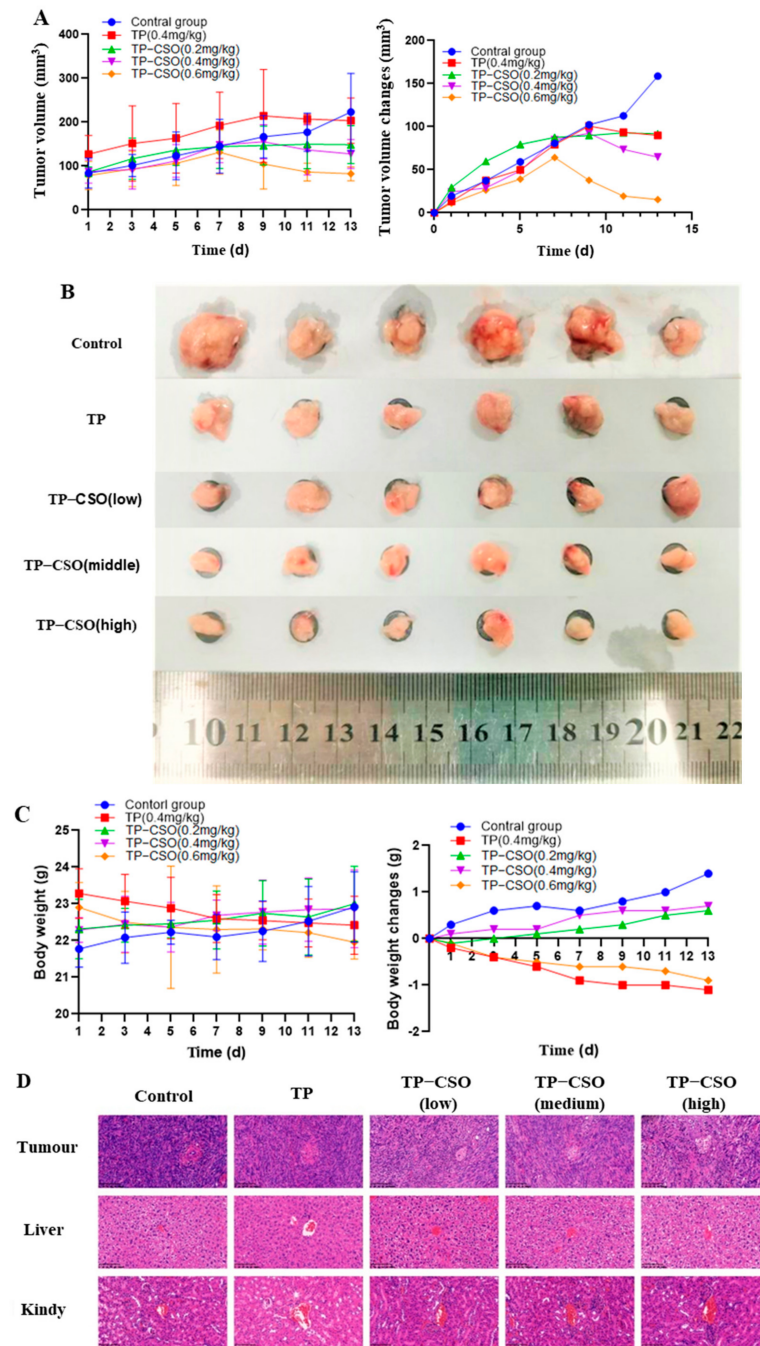


Figure 5. Changes in tumor volume of different drug-treated groups for 14 days (A) and on the last day (B); mouse body weight change with time (C); H&E staining of liver and kidney organs and tumors (D).

In general, body weight in treated groups changes due to a combination of tumor development and drug toxicity. The control group displayed a gradual increase in body weight over 13 days, which showed that the tumor development didn't primarily cause mainly weight loss (Figure 5C). There was no significant difference between the TP-CSO groups

(0.2 and 0.4 mg/kg) and the control group ($p < 0.05$), whereas the TP group (0.4 mg/kg) and the TP-CSO group (0.6 mg/kg) showed an obvious decrease in body weight, indicating the result of the dual effects of both the TP toxicity and its dose dependency. The results suggested that TP-CSO had a better anti-tumor effect and lower in vivo toxicity than TP. We hypothesized that the controlled release of TP-CSO would reduce the instantaneous TP concentration in the blood and prolong the TP circulation time in the blood, which could improve its biological safety and antitumor activity.

As shown in Figure 5D, the control group showed the obvious nuclear division, and negligible apoptosis levels were observed in the dense tumor cells, whereas the treated groups exhibited a large number of cell necrosis and apoptosis in the tumor tissues, indicating TP and TP-CSO have a significant inhibitory effect on tumor cells. In particular, the medium- and high-dose TP-CSO groups displayed a higher apoptosis rate and cell necrosis than the TP group, indicating that TP-CSO has better anti-tumor activity than TP. Analysis of histological staining revealed the obvious kidney proximal tubular dilation and fatty degeneration in the hepatocytes in the TP group (Figure 5D). However, no significant histopathological changes were observed in the TP-CSO groups, which was consistent with the in vivo toxicity results of TP-CSO.

3. Materials and Methods

3.1. Materials

Triptolide was provided by Xi'an Haoxuan Biotechnology Co. Ltd. in Xi'an, China. Chitosan oligosaccharide (CSO, MW: about 3000 Da) was purchased from Aladdin (Beijing, China) and purified using dialysis. Hyclone fetal bovine serum, Trypsin, Dulbecco's Modified Eagle's Medium (DMEM), and Phosphate Buffered Saline (PBS 1X, sterile) were all obtained from Beijing Solarbio Science and Technology Co. Ltd. (Beijing, China). Dimethyl sulfoxide, acetonitrile and methanol were MS-grade reagents provided by Tedia. The water used in the experiments was prepared by a Milli-Q ultrapure water instrument (Millipore, Bedford, MA, USA). Hepatocytes (HL7702) and mouse pancreatic cancer cells (Panco2) were purchased from American type cultures (Manassas, VA, USA). Other chemicals were of commercially available analytical grade.

3.2. Preparation and Characterization of TP-CSO Conjugate

A 2'-hemisuccinic acid derivative of TP (TPS) was prepared according to our previously reported method [19]. In short, 360 mg of TP (1 mmol), 400 mg of succinic anhydride (4 mmol), and 24 mg of 4-dimethylaminopyridine (0.2 mmol) were dissolved in 10 mL of pyridine. The mixture was stirred for 24 h under nitrogen purging at room temperature. After the reaction was completed, the solvent was removed, and the residue was purified by silica gel column chromatography.

TPS: ^1H NMR (500 MHz, DMSO- d_6) δ 12.23 (s, 1H), 4.99–4.95 (m, 1H), 4.89–4.81 (m, 1H), 4.78 (dd, $J = 17.7, 3.5$ Hz, 1H), 3.95 (d, $J = 3.2$ Hz, 1H), 3.71–3.66 (m, 1H), 3.56 (d, $J = 5.6$ Hz, 1H), 2.65–2.53 (m, 2H), 2.52–2.43 (m, 3H), 2.22 (dt, $J = 15.1, 5.9$ Hz, 1H), 2.16–2.07 (m, 1H), 2.00–1.92 (m, 1H), 1.87 (p, $J = 6.9$ Hz, 1H), 1.80 (dd, $J = 15.1, 13.3$ Hz, 1H), 1.36–1.22 (m, 2H), 0.91 (s, 3H), 0.86 (d, $J = 6.9$ Hz, 3H), 0.74 (d, $J = 6.9$ Hz, 3H).

CSO (300 mg, 0.1 mmol) was dissolved in 8 mL of DMSO at 55 °C and cooled down to room temperature after complete dissolution [22]. TPS (100 mg, 0.22 mmol) dissolved in 8 mL of anhydrous DMSO was activated by EDCI (90 mg, 0.46 mmol; 1-ethyl-3-(3-dimethylamino-propyl) carbodiimide hydrochloride) and HOBt (120 mg, 0.88 mmol; N-Hydroxy benzotriazole) for 6 h at room temperature. Subsequently, the activated TP-SUC solution was added into the CSO solution. The mixture was reacted at room temperature for 24 h. The reaction mixture was then dialyzed three times against ultrapure water in a dialysis bag (molecular weight cut-off: 500 Da). The TP-CSO conjugate was lyophilized into a yellowish solid, followed by a rinse with acetone (3 \times). The dried products were characterized using the ^1H NMR and FTIR. The weight percent of TP in TP-CSO was obtained by high-performance liquid chromatography (HPLC) at 218 nm.

TP-CSO: ^1H NMR (500 MHz, D_2O) δ 7.32 (s, 1H), 5.34 (d, $J = 3.6$ Hz, 1H), 4.83 (s, 5H), 4.48 (s, 1H), 4.09 (s, 1H), 3.92 (s, 1H), 3.85 (d, $J = 12.1$ Hz, 8H), 3.75 (d, $J = 9.8$ Hz, 1H), 3.68 (q, $J = 12.5, 9.9$ Hz, 7H), 3.61 (s, 1H), 3.59 (s, 3H), 3.40 (dd, $J = 19.3, 7.2$ Hz, 4H), 3.22 (dd, $J = 10.5, 3.3$ Hz, 1H), 3.14–2.97 (m, 3H), 2.91 (d, $J = 8.1$ Hz, 7H), 2.78 (s, 3H), 2.62 (s, 66H), 2.39 (s, 2H), 2.21 (d, $J = 8.3$ Hz, 1H), 1.97 (s, 5H), 1.95 (d, $J = 4.0$ Hz, 1H), 1.89 (d, $J = 15.0$ Hz, 1H), 1.83–1.77 (m, 1H), 1.46 (s, 1H), 1.28 (s, 2H), 0.98 (t, $J = 7.2$ Hz, 2H), 0.89 (s, 9H), 0.83 (d, $J = 6.9$ Hz, 1H), 0.71 (s, 5H).

3.3. Differential Scanning Calorimetry (DSC)

DSC curves for TP, CSO, TP-CSO and the physical mixture (TP+CSO) were obtained using a DSC 823e instrument (Mettler-Toledo 823e, Greenville, SC, USA). The powder samples of 20 mg were placed under a stream of nitrogen gas and heated from 50 °C to 400 °C at a heating rate of 5 °C/min prior to the analysis.

3.4. X-ray Diffraction (XRD)

Crystalline characteristics of the TP, CSO, TP-CSO and physical mixture (TP+CSO) were investigated by powder X-ray diffraction (D2 PHASER, Bruker Corporation, Karlsruhe, Germany) by a lamp at $\lambda = 1.54$ Å. The scan speed was set at 5 s and at 0.02 of increment. The diffraction pattern was set in the range of 5–50° (2 θ) at 25 °C.

3.5. Determination of TP Loading Capacity

10 mg of TP-CSO was dissolved in 3 mL deionized water and then shocked for 5 min, ultrasonically dissolved for 5 min, and centrifuged at 4000 r/min for 3 min. The supernatant of 300 μL was diluted with 2.7 mL redistilled water and measured by HPLC. Relations between physical quantities are given in the form of equations, as follows:

$$w_{TP} = k * A_{TP} \quad (1)$$

$$\text{TP Loading}(\%) = \frac{W_{TP}}{W_{TP-CSO}} \times 100\% \quad (2)$$

the peak area of TP was represented with A_{TP} . The linear relation between the peak area and concentration of TP was represented with k . The weight of TP-CSO and TP were represented with W_{TP-CSO} and W_{TP} , respectively. The drug loading capacity was calculated according to Equation (2).

3.6. The Water Solubility Study

For the water solubility studies, TP-CSO (30 mg) was dissolved in 1.0 mL ultrapure water. The mixture was treated using ultrasonic waves for 15 min, vortexed for 3 min, and centrifuged at 12,000 rpm for 10 min. Saturated supernatants were quantified by UV-vis spectrophotometer at 218 nm excited wavelength.

3.7. In Vitro Release Study of TP-CSO

To investigate the release of TP-CSO, we assessed the stability of TP-CSO under various conditions. Briefly, TP-CSO (8 mg) was dissolved in 2.0 mL of the mouse plasma, cell culture medium (Containing 10% FBS) and simulated gastric juice (SGF; 0.32% pepsin, pH 1.2) as well as simulated intestinal fluid (SIF; 1% trypsin, pH 7.5), respectively. 100 μL samples were taken after 0.5, 1, 2, 4, 8, 12 and 24 h of incubation at 37 °C, and extraction of 200 μL of dichloromethane. HPLC was performed on an Agilent C-18 column (4.6 \times 250 mm, 5 μm) with acetonitrile/water (33:67, 1 mL/min) as mobile phase.

3.8. Pharmacokinetic Study

To evaluate the in vivo pharmacokinetics of TP-CSO conjugate, the SD rats (250–300 g, Sprague-Dawley rat) fasted 12 h in advance and were randomized into two groups ($n = 5$) and respectively treated with TP (0.4 mg/kg) and TP-CSO (0.4 mg/kg, TP equivalent). The

blood samples (500 μ L) were collected through the ocular chorionic vein at 5, 15, 30, 60, 120, 180, 240, 360, 480 and 720 min after intragastric administration. Subsequently, the samples were immediately centrifuged at 3500 rpm for 15 min. An upper plasma sample was collected and kept at -80 $^{\circ}$ C.

Sample processing: to the plasma sample, 10 μ L of ferulic acid (2.5 ng/mL) was added as internal standard. The sample (100 μ L) was placed in a 1.5 mL Eppendorf tube, to which 800 μ L of ethyl acetate was added and vortexed for 3 min, and this was centrifuged at 12,000 rpm for 15 min. The upper solution was taken and blow dried with nitrogen at room temperature. The dried residue was dissolved in 100 μ L of methanol-water (60:40, *v/v*) solution, vortexed for 3 min, subsequently centrifuged at 12,000 rpm for 15 min at 4 $^{\circ}$ C and the upper solution was collected into a 2 mL vial.

10 μ L of sample was injected into a Waters C-18 column (2.1 mm \times 50 mm, 1.8 μ m) on a Sciex X500R QTOF Mass Spectrometer (UPLC-MS; Framingham, MA, USA). The column was eluted with methanol (A)/water (B) solution at a flow rate of 0.3 mL/min and a column temperature of 35 $^{\circ}$ C (0–6 min, A: 40%–90%; 6–8.1 min, A: 90%; 8.1–10 min, A: 40%). The operating conditions of UPLC-MS are as follows: electrospray ionization source (ESI), negative ionization mode; Ion spray voltage (ISV), 3500 V; Drying temperature, 325 $^{\circ}$ C; Flow rate of desolvent gas, 8.0 L/min; Atomization temperature, 350 $^{\circ}$ C. The pyrolysis energy and impact energy of TP were 120 V and 10 V, respectively, and those of ferulic acid were 90 V and 10 V, respectively. A multiple reaction monitoring mode (MRM) was used to monitor the transformation of TP from *m/z* [M-H] 359.1 \rightarrow 241.1 and ferulic acid *m/z* [M-H] 193.1 \rightarrow 134.1 to productions.

3.9. In Vivo Toxicity Study

The 30 normal C57 mice (20–25 g) were randomly divided into a normal saline group, TP (0.4 mg/kg) group and TP-CSO group (equivalent TP of 0.2, 0.4 and 0.6 mg/kg), respectively. The drugs were administered by a gavage once every two days for seven times. The body weight and fatality rate were recorded daily. On the 14th day, blood was collected from the eyes, and the organs were harvested after the mice were euthanized. A Beckman CX5 automated analyzer detected renal function indexes, liver function indexes (serum alanine aminotransferase (ALT), aspartic aminotransferase (AST)), and (blood urea nitrogen (BUN) creatinine (CRE)).

3.10. In Vivo Antitumor Study

The antitumor activity of the TP-CSO conjugate was evaluated on Panco2 tumor-bearing mice. First, C57 mice (20–25 g) were implanted subcutaneously with 2×10^6 Panco2 cells. When the tumor grew up to about 100 mm³, the mice were orally administrated with 0.4 mg/kg TP and TP-CSO (0.2, 0.4 and 0.6 mg TP equivalent/kg) once every two days, respectively. The body weight and fatality rate were recorded. Mice in control groups were orally administrated with saline solution. The tumor volume was measured with calipers and calculated by the $(1/2)(a \times b^2)$ formula (*a* is long diameter, *b* is short diameter). After 14 days of intragastric administration, the mice were sacrificed, and livers, kidney, and tumors were harvested.

3.11. Statistical Analysis

All the data in this study were presented as mean and standard deviation. Differences among groups of data were compared by student's *t*-test or analysis of variance. A value of $p < 0.05$ was considered significant.

4. Conclusions

A TP-CSO prodrug was synthesized and characterized by ¹H NMR, FTIR spectrum, DSC and XRD analysis. TP-CSO exhibited over a 35-fold water solubility (15 mg/mL) in comparison with TP. The bioavailability of TP-CSO after oral administration was higher than the parent TP along with the prolonged circulation time in the blood. Consequently,

compared with the same dose of TP, TP-CSO has lower toxicity and a more potent tumor-suppressive effect, showing significant potential for further clinical trials. In conclusion, the CSO-based conjugate system may be useful as a platform for oral delivery of other sparingly soluble drugs.

Supplementary Materials: The following supporting information can be downloaded at: <https://www.mdpi.com/article/10.3390/molecules27123686/s1>, Figure S1: ¹H NMR spectra of TPS, CSO and TP-CSO; Figure S2: Standard curve for TP; Figure S3: HPLC spectra of TP weight percentage in TP-CSO (sig = 218, 4).

Author Contributions: Conceptualization, X.W. (Xinlong Wang) and H.Z.; Writing—original draft preparation, X.W. (Xinlong Wang); Writing—review and editing, X.W. (Xinlong Wang) and H.Z.; visualization, X.W. (Xinlong Wang); Project administration, X.W. (Xiangxiang Wu) and M.M.; Funding acquisition, X.W. (Xiangxiang Wu) and H.Z. All authors have read and agreed to the published version of the manuscript.

Funding: This project was sponsored by National Natural Science Foundation of China (21601053, U1604185), Henan Scientific and technological Innovation Talents Project (20HASTIT050), Henan Science Fund for Excellent Young Scholars (212300410057), Henan Scientific Research Funding Project for Overseas Staffs 2020 (No: 29), Natural Science Foundation of Henan Province (222300420482).

Institutional Review Board Statement: The animal study protocol was approved by the Experimental Animal Ethics Committee of Henan University of Chinese Medicine (Approval ID: DWLL201903010).

Informed Consent Statement: Not applicable.

Data Availability Statement: The data presented in this study are available upon request from the corresponding author.

Acknowledgments: The authors are grateful to Ning Sun (Henan University of Chinese Medicine) technical assistance with TEM analysis.

Conflicts of Interest: The authors declare that they have no competing financial interests.

References

1. McGuigan, A.; Kelly, P.; Turkington, R.C.; Jones, C.; Coleman, H.G.; McCain, R.S. Pancreatic cancer: A review of clinical diagnosis, epidemiology, treatment and outcomes. *World J. Gastroenterol.* **2018**, *24*, 4846–4861. [[CrossRef](#)] [[PubMed](#)]
2. Jentzsch, V.; Davis, J.; Djamgoz, M. Pancreatic Cancer (PDAC): Introduction of Evidence-Based Complementary Measures into Integrative Clinical Management. *Cancers* **2020**, *12*, 3096. [[CrossRef](#)] [[PubMed](#)]
3. Mizrahi, J.D.; Surana, R.; Valle, J.W.; Shroff, R.T. Pancreatic cancer. *Lancet* **2020**, *395*, 2008–2020. [[CrossRef](#)]
4. Conroy, T.; Hammel, P.; Hebbar, M.; Ben Abdelghani, M.; Wei, A.C.; Raoul, J.L.; Choné, L.; Francois, E.; Artru, P.; Biagi, J.J.; et al. FOLFIRINOX or Gemcitabine as Adjuvant Therapy for Pancreatic Cancer. *N. Engl. J. Med.* **2018**, *379*, 2395–2406. [[CrossRef](#)] [[PubMed](#)]
5. Lee, Y.S.; Lee, J.C.; Kim, J.H.; Kim, J.; Hwang, J.H. Pharmacoefficacy of FOLFIRINOX versus gemcitabine plus nab-paclitaxel in metastatic pancreatic cancer: A systematic review and meta-analysis. *Sci. Rep.* **2021**, *11*, 20152. [[CrossRef](#)] [[PubMed](#)]
6. Saung, M.T.; Zheng, L. Current Standards of Chemotherapy for Pancreatic Cancer. *Clin. Ther.* **2017**, *39*, 2125–2134. [[CrossRef](#)]
7. Hackert, T.; Sachsenmaier, M.; Hinz, U.; Schneider, L.; Michalski, C.W.; Springfield, C.; Strobel, O.; Jäger, D.; Ulrich, A.; Büchler, M.W. Locally Advanced Pancreatic Cancer: Neoadjuvant Therapy With Folfirinox Results in Resectability in 60% of the Patients. *Ann. Surg.* **2016**, *264*, 457–463. [[CrossRef](#)]
8. Li, J.X.; Shi, J.F.; Wu, Y.H.; Xu, H.T.; Fu, C.M.; Zhang, J.M. Mechanisms and application of triptolide against breast cancer. *Zhongguo Zhong Yao Za Zhi* **2021**, *46*, 3249–3256.
9. Shi, J.; Ren, Y.; Ma, J.; Luo, X.; Li, J.; Wu, Y.; Gu, H.; Fu, C.; Cao, Z.; Zhang, J. Novel CD44-targeting and pH/redox-dual-stimuli-responsive core-shell nanoparticles loading triptolide combats breast cancer growth and lung metastasis. *J. Nanobiotech.* **2021**, *19*, 188. [[CrossRef](#)]
10. Hu, H.; Huang, G.; Wang, H.; Li, X.; Wang, X.; Feng, Y.; Tan, B.; Chen, T. Inhibition effect of triptolide on human epithelial ovarian cancer via adjusting cellular immunity and angiogenesis. *Oncol. Rep.* **2018**, *39*, 1191–1196. [[CrossRef](#)]
11. Giri, B.; Gupta, V.K.; Yaffe, B.; Modi, S.; Roy, P.; Sethi, V.; Lavania, S.P.; Vickers, S.M.; Dudeja, V.; Banerjee, S.; et al. Pre-clinical evaluation of Minnelide as a therapy for acute myeloid leukemia. *J. Transl. Med.* **2019**, *17*, 163. [[CrossRef](#)] [[PubMed](#)]
12. Zhou, Z.L.; Yang, Y.X.; Ding, J.; Li, Y.C.; Miao, Z.H. Triptolide: Structural modifications, structure-activity relationships, bioactivities, clinical development and mechanisms. *Nat. Prod. Rep.* **2012**, *29*, 457–475. [[CrossRef](#)] [[PubMed](#)]

13. Zhu, W.; Li, J.; Wu, S.; Li, S.; Le, L.; Su, X.; Qiu, P.; Hu, H.; Yan, G. Triptolide cooperates with Cisplatin to induce apoptosis in gemcitabine-resistant pancreatic cancer. *Pancreas* **2012**, *41*, 1029–1038. [[CrossRef](#)] [[PubMed](#)]
14. Li, X.; Mao, Y.; Li, K.; Shi, T.; Yao, H.; Yao, J.; Wang, S. Pharmacokinetics and tissue distribution study in mice of triptolide-loaded lipid emulsion and accumulation effect on pancreas. *Drug Deliv.* **2016**, *23*, 1344–1354. [[CrossRef](#)]
15. Patil, S.; Lis, L.G.; Schumacher, R.J.; Norris, B.J.; Morgan, M.L.; Cuellar, R.A.; Blazar, B.R.; Suryanarayanan, R.; Gurvich, V.J.; Georg, G.I. Phosphonoxyethyl Prodrug of Triptolide: Synthesis, Physicochemical Characterization, and Efficacy in Human Colon Adenocarcinoma and Ovarian Cancer Xenografts. *J. Med. Chem.* **2015**, *58*, 9334–9344. [[CrossRef](#)]
16. Zhou, Y.; Xia, L.; Yao, W.; Han, J.; Wang, G. Arctiin Antagonizes Triptolide-Induced Hepatotoxicity via Activation of Nrf2 Pathway. *Biomed. Res. Int.* **2020**, *2020*, 2508952. [[CrossRef](#)]
17. Xie, L.; Zhao, Y.; Duan, J.; Fan, S.; Shu, L.; Liu, H.; Wang, Y.; Xu, Y.; Li, Y. Integrated Proteomics and Metabolomics Reveal the Mechanism of Nephrotoxicity Induced by Triptolide. *Chem. Res. Toxicol.* **2020**, *33*, 1897–1906. [[CrossRef](#)]
18. Xu, Y.; Fan, Y.F.; Zhao, Y.; Lin, N. Overview of reproductive toxicity studies on *Tripterygium wilfordii* in recent 40 years. *Zhongguo Zhong Yao Za Zhi* **2019**, *44*, 3406–3414.
19. Lee, E.; Kim, H.; Lee, I.H.; Jon, S. In vivo antitumor effects of chitosan-conjugated docetaxel after oral administration. *J. Control. Release* **2009**, *140*, 79–85. [[CrossRef](#)]
20. Lee, E.; Lee, J.; Lee, I.H.; Yu, M.; Kim, H.; Chae, S.Y.; Jon, S. Conjugated chitosan as a novel platform for oral delivery of paclitaxel. *J. Med. Chem.* **2008**, *51*, 6442–6449. [[CrossRef](#)]
21. Zeng, H.; Zhu, X.; Tian, Q.; Yan, Y.; Zhang, L.; Yan, M.; Li, R.; Li, X.; Wang, G.; Ma, J.; et al. In vivo antitumor effects of carboxymethyl chitosan-conjugated triptolide after oral administration. *Drug Deliv.* **2020**, *27*, 848–854. [[CrossRef](#)] [[PubMed](#)]
22. Lee, J.Y.; Termsarasab, U.; Lee, M.Y.; Kim, D.H.; Lee, S.Y.; Kim, J.S.; Cho, H.J.; Kim, D.D. Chemosensitizing indomethacin-conjugated chitosan oligosaccharide nanoparticles for tumor-targeted drug delivery. *Acta Biomater.* **2017**, *57*, 262–273. [[CrossRef](#)] [[PubMed](#)]
23. Kittur, F.S.; Prashanth, K.V.H.; Sankar, K.U.; Tharanathan, R.N. Characterization of chitin, chitosan and their carboxymethyl derivatives by differential scanning calorimetry. *Carbohydr. Polym.* **2002**, *49*, 185–193. [[CrossRef](#)]
24. Xi, C.; Peng, S.; Wu, Z.; Zhou, Q.; Zhou, J. Toxicity of triptolide and the molecular mechanisms involved. *Biomed. Pharmacother.* **2017**, *90*, 531–541. [[CrossRef](#)] [[PubMed](#)]